

Control of thermal conduction and rectification in a model of complex networks with two asymmetric parts


Kezhao Xiong,^{1,2} Jie Zhou,¹ Ming Tang,¹ Chunhua Zeng,^{3,2,4,*} and Zonghua Liu^{1,†}

¹*Department of Physics, East China Normal University, Shanghai 200062, People's Republic of China*

²*Department of Mechanical Engineering, University of Colorado Boulder, Colorado 80309, USA*

³*Institute of Physical and Engineering Science, Kunming University of Science and Technology, Kunming 650500, People's Republic of China*

⁴*Department of Physics, Tsinghua University, Beijing 100084, People's Republic of China*

 (Received 26 October 2018; revised manuscript received 28 November 2018; published 28 December 2018)

The controlling of heat flux is an important topic in the field of heat conduction and has potential applications in thermal devices. We here design a model of asymmetric network structure to study this problem in complex networks, which is composed of two parts with different topologies. We find that the heat conduction and rectification can be significantly changed by adjusting two parameters: the network rewiring parameter δ and coupling parameter λ . Two typical network structures are considered. One is composed of a random network and a two-dimensional regular lattice with half by half. Another is composed of two random networks with opposite coupling parameter $\pm\lambda$. Our numerical simulations show that for the first case, both the network flux and rectification coefficient decrease monotonically with the increase of δ and there is an optimal λ for the maximum flux. For the second case, the network flux will decrease monotonically while the rectification coefficient increases monotonically, with the increase of λ . A brief theory of phonon spectra is applied to explain the numerical results.

DOI: [10.1103/PhysRevE.98.062144](https://doi.org/10.1103/PhysRevE.98.062144)

I. INTRODUCTION

Low-dimensional nanoscale systems have been extensively studied due to their promising potential applications for future phononic or thermal devices in the last few decades [1–8], which include thermal rectification [3,4,9,10], thermal logic gates [11,12], negative differential thermal resistance, thermal transistors [13,14], etc. These studies have raised an exciting prospect of using these materials in thermal devices [15,16]. Especially, the possibility of designing a thermal diode by coupling three nonlinear chains was reported [17]. Inspired by these theoretical studies [9,17], Chang and co-workers have produced a microscopic solid-state thermal rectifier, based on carbon nanotubes [18]. On the other hand, DNA is another one of the most promising nanotube and nanowire materials due to the relative ease of modifications combined with the self-assembly capability, which make it possible to construct a great variety of DNA-based nanostructures [19–26], such as tunable thermal switching via DNA-based nanodevices [27], thermal diodes, and heat pumps based on DNA nanowires [28]. These fundamental works mainly focus on the thermal properties of individual lattice nanostructures such as a one-dimensional (1D) lattice or a single nanowire or nanotube. However, for practical applications, a single nanowire or nanotube is extremely difficult to assemble and to control and manipulate. Instead, researchers generally try to make devices from networks of nanowires and nanotubes [29],

which provide applications in many fields, such as large-scale transparent conductors, transistors, sensors, and even flexible electronics [30,31].

Among them [32–35], electrical conduction of complex networks has been extensively studied. For example, it is shown that electric transport changes linearly with the number of added bonds [36], the heterogeneity of complex networks enables fast mutual access of all nodes and thus improves electric transport [37], and the electric resistance of network can be figured out by the Kirchhoff second law for the complicated parallel and serial electric circuits [38]. However, the corresponding thermal properties of complex networks remain largely unexplored, in contrast to these studies of electrical conduction. In an oversimplified network model [39,40], it is found that the interface thermal resistance depends sensitively on the strength of coupling between coupled chains [39], and the heat conduction of network decreases with the increase of heterogeneity of network caused by both the degree distribution and clustering coefficient [40]. Recently we extended the network model to a more realistic situation where network links are represented by 1D chains of atoms [41], in contrast to the simplified springs in Ref. [40]. These findings indicate that there are essential differences between the electric conduction transferred by electrons and heat conduction transferred by lattice vibrations.

In thermal devices, a key problem is how to control and manipulate heat conduction. To study this problem in thermal devices with the structure of complex networks [29–31], especially the network of three-dimensional random array of nanotubes [42], we here present a model of complex networks rewired from a two-dimensional (2D) regular lattice and focus

*chzeng83@kmust.edu.cn

†zhliu@phy.ecnu.edu.cn

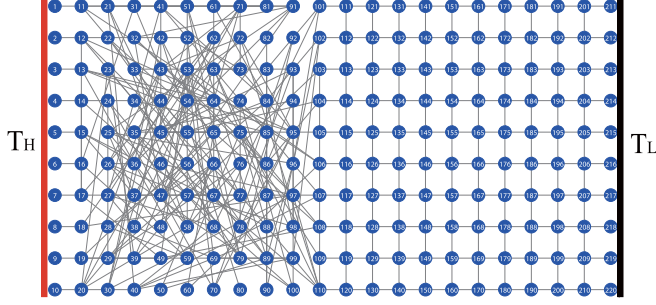


FIG. 1. Schematic of the network structure from a 2D lattice, where the left part is rewired by the rewiring approach [34,46] and the right part remains as a 2D lattice. The nodes of both the first column at left and that of the last column at right are in contact with the thermal baths with higher temperature T_H and lower temperature T_L , respectively.

on how the thermal properties are affected by topological structures. Two typical cases are considered. One is composed of a part of a random network and a part of 2D regular lattice, with half by half. The other is composed of two random networks with opposite coupling parameter $\pm\lambda$. We find that the heat flux of network can be adjusted by two parameters: the rewiring parameter δ and coupling parameter λ . There is a rectification effect of heat flux in both cases, which is possible only in the smaller controlling parameter δ . The rectification effect will be reversed when the coupling parameter λ changes. A brief theory of phonon spectra is applied to explain the numerical results.

The remainder of the paper is organized as follows. In Sec. II we present a model of complex network to study the rectification, which is composed of two asymmetric parts. In Sec. III we make extensive numerical simulations to study the controlling of thermal conduction and rectification. In Sec. IV we give a brief theoretical analysis. Finally, in Sec. V we give conclusions and discussions.

II. A RECTIFICATION MODEL OF COMPLEX NETWORK WITH TWO ASYMMETRIC PARTS

We first construct a 2D lattice with $N = 2(m + 1) \times m$ nodes and let the nodes of the first column at left and the nodes of the last column at right contact the thermal baths with higher temperature T_H and lower temperature T_L , respectively, as shown in the schematic Fig. 1. The nodes contacted to the thermal baths are disconnected with each other. We let the two thermal baths be the Nose-Hoover thermostat [43,44] with T_H and T_L , respectively. For convenience of discussion, we let each node have a number i with $i = 1, 2, \dots, N$; see Fig. 1 for details.

Then we divide the 2D lattice into two equal parts and change the structure of the left part into a random network by the rewiring approach [34,45,46]; see Fig. 1 for a typical rewired structure. In detail, for each link in the left part of a 2D lattice, we randomly fix its one end i and rewire its another end to a new node j in the same left part of a 2D lattice, according to the probability

$$P_{i,j} \sim r_{i,j}^{-\delta}, \quad (1)$$

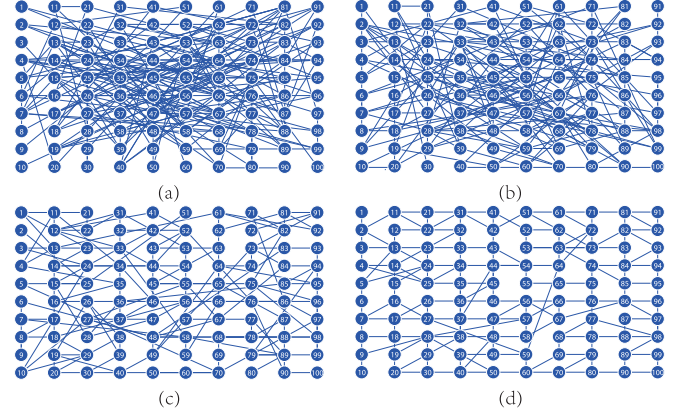


FIG. 2. How the parameter δ influences the structure of the rewired part in Fig. 1, where only the left part of Fig. 1 is shown and panels from (a) to (d) represent four typical cases with $\delta = 0.0, 1.0, 2.0$, and 4.0 , respectively.

where $r_{i,j}$ represents the Euclidean distance between the nodes i and j and the exponent δ is a controlling parameter [46–48]. The larger the parameter δ , the shorter the average link length. Figure 2 shows the rewired structures for the left part in Fig. 1 where panels (a)–(d) represent four typical cases with $\delta = 0.0, 1.0, 2.0$, and 4.0 , respectively. We see that with the increase of δ , the network will change gradually from a completely random network in Fig. 2(a) to an approximate regular network in Fig. 2(d). We have to pointed out that $r_{i,j}$ is measured on the assumption that $r_{i,j} = 1$ for two neighboring nodes in a regular 2D lattice.

Following Ref. [40], we let each node of Fig. 1 represent an atom and each link between two neighboring nodes be a nonlinear spring with the Hamiltonian

$$H = \sum_i \left[\frac{1}{2} p_i^2 + V_i(x_i) \right], \quad (2)$$

where x_i represents the displacement from the equilibrium position of the i th atom. We let k_i represent the degree of node i , which will be distributed in the left part of Fig. 1 but a constant in the right part of Fig. 1: $k_i = 4$ for the inner nodes and $k_i = 3$ for the boundary nodes. The potential of node i can be given as

$$V_i(x_i) = \frac{1}{2} \sum_{j=1}^{k_i} C_{i,j} \left[\frac{1}{2} (x_i - x_j)^2 + \frac{\varepsilon}{4} (x_i - x_j)^4 \right], \quad (3)$$

where x_j represents the displacement from the equilibrium position of the j th atom, $C_{i,j}$ is the coupling strength for the link between the nodes i and j , the sum is for all the nearest neighboring nodes j of node i , and $\varepsilon = 0.1$ throughout this paper [44]. To reflect the fact that coupling strength is generally decayed with the increase of $r_{i,j}$, we here assume that $C_{i,j}$ depends on the distance $r_{i,j}$ by

$$C_{i,j} = r_{i,j}^{-\lambda}, \quad (4)$$

where the exponent λ represents the controlling parameter of coupling strength. It is easy to notice that we have $C_{i,j} = 1$ for all the links in the right part of Fig. 1 as their $r_{i,j} = 1$. In this work, we will discuss how the two parameters δ and λ

influence the heat conduction and rectification in the network of Fig. 1.

The motion of nodes can be represented as follows. For the source nodes of the first and last columns in Fig. 1, they are in contact with the high- and low-temperature thermal baths T_H and T_L , respectively, and thus they satisfy

$$\dot{p}_H = -\chi_H x_H - \frac{\partial H}{\partial x_H}, \quad \dot{x}_H = \frac{\partial H}{\partial p_H}, \quad (5)$$

$$\dot{p}_L = -\chi_L x_L - \frac{\partial H}{\partial x_L}, \quad \dot{x}_L = \frac{\partial H}{\partial p_L}, \quad (6)$$

where $\dot{\chi}_H = \dot{x}_H^2/T_H - 1$, and $\dot{\chi}_L = \dot{x}_L^2/T_L - 1$. The other atoms satisfy the canonical equations

$$\dot{p}_i = -\frac{\partial H}{\partial x_i}, \quad \dot{x}_i = \frac{\partial H}{\partial p_i}. \quad (7)$$

After the transient process, the network will reach a stationary state. The local temperature at each atom [5] can be defined as

$$T(i) = \langle p_i^2 \rangle, \quad (8)$$

and the heat flux along a link is

$$J_i = \langle \dot{x}_i \partial V / \partial x_{i+1} \rangle. \quad (9)$$

The total heat flux of network, J , will be the sum of all the J_i from the source nodes with high-temperature T_H to the source nodes with low-temperature T_L . Considering the asymmetric structure of Fig. 1, we let J_+ be the total heat flux from left to right. Then we switch the temperatures T_H and T_L and let J_- be the total heat flux from right to left. Generally, J_+ and J_- will be different, and their difference represents the thermal rectification, which is one important physical phenomenon [9]. This nonreciprocal transport phenomenon has been confirmed in many nanostructure systems [5,49,50]. The rectification coefficient can be defined as [40]

$$R_e = \frac{|J_+ - J_-|}{\max(J_+, J_-)}. \quad (10)$$

III. NUMERICAL SIMULATIONS

In numerical simulations, we let $m = 16$, $T_H = 6.0$, and $T_L = 2.0$, if without specific illustration. We take the transient process as the integration of 10^6 dimensionless time units with a time step of 0.01. After that, the network will reach a stationary state. Then we calculate the total heat flux J_{\pm} for different δ and λ . Figures 3(a) and 3(b) show the dependences of J_{\pm} and R_e on δ for $\lambda = 0$, respectively. From Fig. 3(a) we see that the heat flux J_{\pm} decreases monotonically with the increase of δ and has a maximum at $\delta = 0.0$. The possible reason is that for the case of $\delta = 0.0$, the left part of Fig. 1 is a completely random network with the minimum average shortest path of network [51], which enhances the heat conduction of network. When δ increases, the possibility for long links will be reduced and the average shortest path of network will increase, resulting in the decrease of J_{\pm} . From Fig. 3(b) we see that R_e also decreases monotonically with the increase of δ and has a maximum at $\delta = 0.0$. The reason is that the structure difference between the left and right parts of Fig. 1 is a maximum for the case of $\delta = 0.0$. As the asymmetry

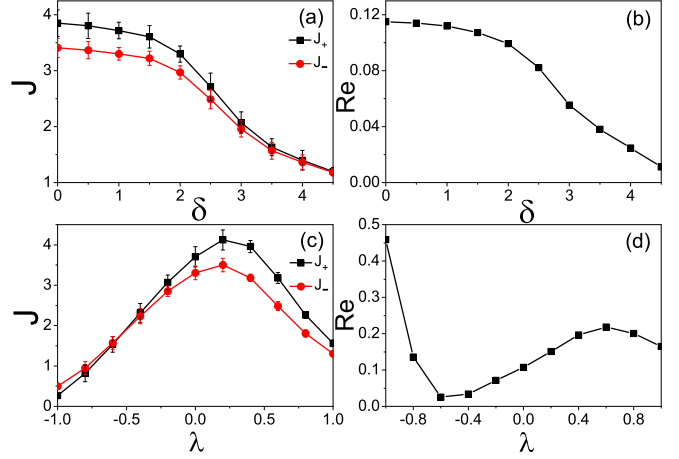


FIG. 3. Dependence of J_{\pm} and R_e on the two parameters δ and λ for averaging on 40 realizations. (a, b) The case of $\lambda = 0.0$. (a) J_{\pm} vs δ ; (b) R_e vs δ . (c, d) The case of $\delta = 0.0$. (c) J_{\pm} vs λ ; (d) R_e vs λ .

between the left and right parts of Fig. 1 is the main reason to make the difference between J_+ and J_- , the decrease of this asymmetry will reduce the difference between J_+ and J_- and thus results in the decrease of R_e .

Similarly, Figs. 3(c) and 3(d) show the dependences of J_{\pm} and R_e on λ for $\delta = 0$, respectively. They are both nonmonotonously, in contrast to the monotonous decrease in Figs. 3(a) and 3(b). From Fig. 3(c) we see that there is an optimal maximum J_{\pm} at around $\lambda \approx 0.25$. The reason is that the increase of λ will enhance the transport of heat energy and also change the interface thermal resistance, which is an intrinsic factor of heat conduction in network and depends sensitively on the strength of coupling [39,40]. The competition between these two quantities of coupling strength and interface thermal resistance makes the crossover of J_{\pm} , which also works for the explanation of R_e . A quantitative explanation will be given later with the theory of phonon spectra.

To understand the results of Fig. 3 better, we show its temperature distributions for two typical network structures of $\delta = 0.0$ and 4.5 in Figs. 4(a) and 4(b), respectively, which correspond to the two extreme cases of a random network and approximate regular 2D network for the left part of Fig. 1, respectively. Three features can be noticed in Figs. 4(a) and 4(b). The first one is that the temperature distributions in the right part of Figs. 4(a) and 4(b) show a gradient change, which comes from the homogeneous structure of a regular 2D lattice and is consistent with Fourier's law. The second one is that there are more peaks in the left part of Fig. 4(a) than that in Fig. 4(b). The reason is that the left part of Fig. 4(a) is a random network and thus has more long links than that of the approximate regular 2D lattice of Fig. 4(b). It was pointed out that the long links will usually generate the platforms of approximately equal temperatures among remote nodes [39,40], which result in more peaks in Fig. 4(a) than that in Fig. 4(b). The third one is the jumping of temperature difference nearby the source nodes. We see that the jumping amplitude is significantly different between Figs. 4(a)

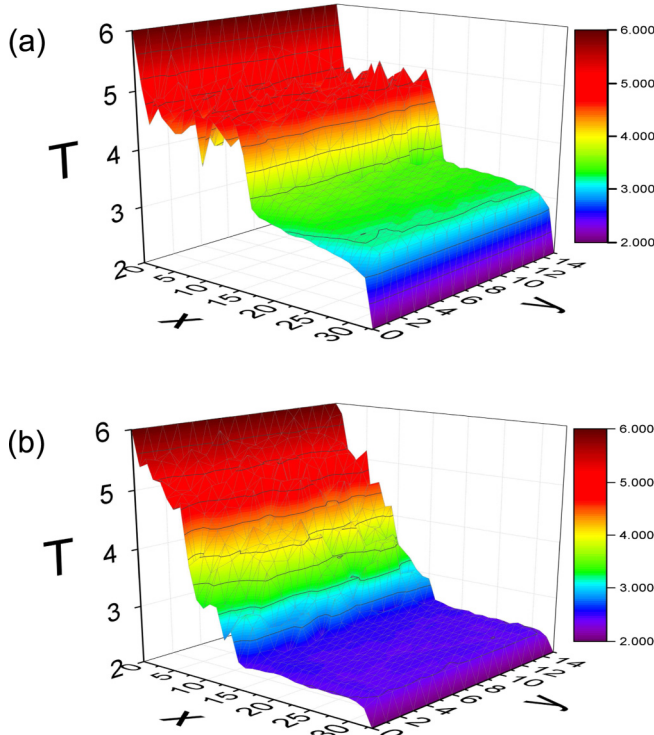


FIG. 4. Temperature distributions for the network in Figs. 3(a) and 3(b) with $\lambda = 0.0$ where δ takes 0.0 (a) and 4.5 (b).

and 4(b), confirming the influence of the interface thermal resistance.

The above rectification effect is caused by rewiring only the left half of network. An intuitive question is what about rewiring both the left and right parts of network. To figure out the answer, we rewire both the left and right parts of network independently. Then we let the coupling parameter λ be opposite for the two parts: we have a positive $\lambda > 0.0$ for the left half of network and an equal but negative $-\lambda$ for the right half of network. Figures 5(a) and 5(b) show the rewiring case of $\delta = 0.0$ where (a) and (b) represent the dependences of J_{\pm} and R_e on λ , respectively. We see that with the increase of λ , the heat flux J_{\pm} decreases monotonically, while the rectification coefficient R_e increases monotonically. Comparing Figs. 5(a) and 5(b) with Figs. 3(c) and 3(d), respectively, we find two different points. One is that the behaviors of both J_{\pm} and R_e are monotonous in Figs. 5(a) and 5(b) but nonmonotonous in Figs. 3(c) and 3(d). The other is that the varying range of J_{\pm} in Fig. 5(a) is much smaller than that in Fig. 3(c), and the varying range of R_e in Fig. 5(b) is much larger than that in Fig. 3(d). We will explain it more in the next section.

The above results are obtained for fixed $T_H = 6.0$ and $T_L = 2.0$. It will be interesting to check whether they depend on the temperatures of source nodes. For this purpose, we have considered other temperatures and found that the conclusions remain unchanged. Figures 5(c) and 5(d) show the results for $T_H = 0.6$ and $T_L = 0.2$, where the other parameters remain the same as in Figs. 5(a) and 5(b). Comparing Figs. 5(c) and 5(d) with Figs. 5(a) and 5(b), respectively, we see that they have the similar variation tendency, confirming that the effect

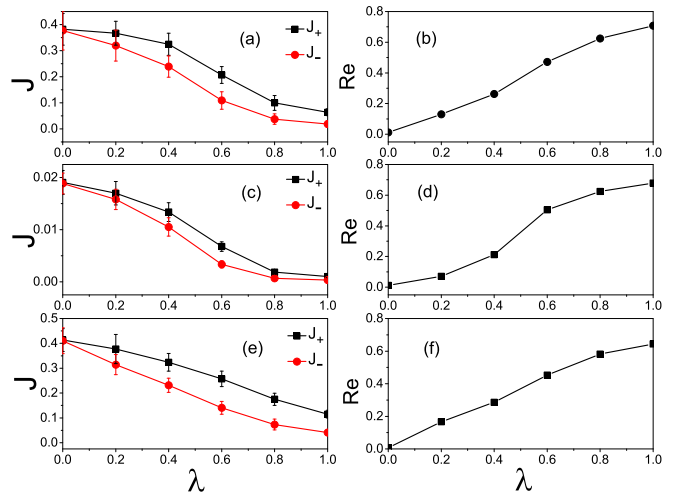


FIG. 5. Case of rewiring both the left and right parts of network. Dependence of J_{\pm} and R_e on λ for $\delta = 0.0$ and averaged on 40 realizations. (a, b) The case of $T_H = 6.0$ and $T_L = 2.0$ with the Nose-Hoover heat baths; (c, d) the case of $T_H = 0.6$ and $T_L = 0.2$ with the Nose-Hoover heat baths; and (e, f) the case of $T_H = 6.0$ and $T_L = 2.0$ with the Langevin heat baths.

of rectification is independent of the temperatures of source nodes.

On the other hand, it will be also interesting to check whether the obtained results depend on the thermal baths. For this purpose, we replace the Nose-Hoover thermostat by the stochastic Langevin thermostat [5,41]. Figures 5(e) and 5(f) show the results, where the other parameters remain the same as in Figs. 5(a) and 5(b). Comparing Figs. 5(e) and 5(f) with Figs. 5(a) and 5(b), respectively, we see that they are qualitatively the same as each other, confirming that the effect of rectification is also independent of the heat baths.

IV. A BRIEF THEORETICAL ANALYSIS

We now first use the theory of phonon spectra [9] to explain the rectification in Figs. 3(c) and 3(d). From Fig. 1 we see that the asymmetry of network mainly comes from the interface nodes between the left and right parts of network. For comparison, we choose the interface nodes with the same degree $k_i = 4$, one from the left part and the other from the right part of network. We plot their power spectra in Fig. 6 with $\delta = 0.0$, where Figs. 6(a) and 6(b) represent the cases of $\lambda = 1.0$ and -1.0 , respectively. We see that for the case of $\lambda = 1.0$ in Fig. 6(a), the bandwidths of power spectra of these two interface nodes are different: the case of the left interface node is narrower than that of the right interface node. On the other hand, for the case of $\lambda = -1.0$, the bandwidths of the power spectra of these two interface nodes are inverse, i.e., the case of the left interface node is larger than that of the right interface node. Thus, in the case of $\lambda = 1.0$, the phonon diffusion is from narrow frequency to wide frequency. As the narrow phonon band is within the wide phonon band, it is easy for the phonon to flow from T_H to T_L , which results in $J_+ > J_-$, but for the case of $\lambda = -1.0$, the phonon diffusion is from wide frequency to narrow frequency. In this case, only part of the wide phonon band overlaps with the narrow phonon

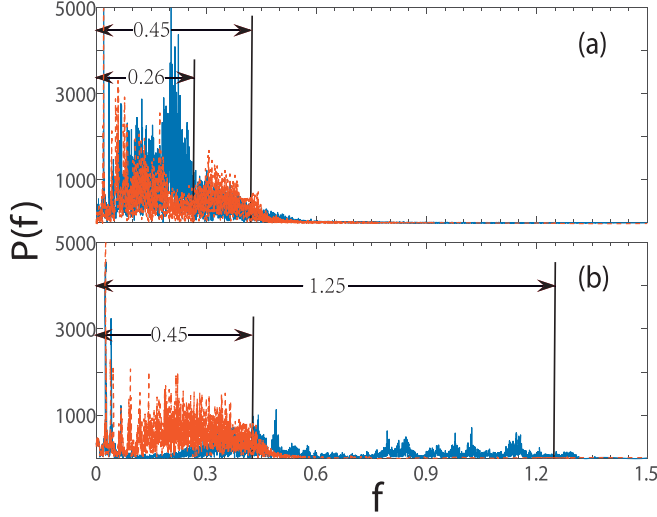


FIG. 6. Power spectra of the interface nodes with the same degree $k_i = 4$ and $\delta = 0.0$ where the blue and red lines represent the cases of the left and right interface nodes, respectively. Panels (a) and (b) represent the cases of $\lambda = 1.0$ and -1.0 , respectively.

band, and thus only part of the phonon can be sent from T_H to T_L , which results in $J_+ < J_-$. Thus, the rectification effects will be reversed when λ increases from 1.0 to -1.0 . Moreover, the overlapped bandwidth is larger for the case of $\lambda = 1.0$ than that of $\lambda = -1.0$, resulting in that the value of R_e of $\lambda = 1.0$ is smaller than that of $\lambda = -1.0$.

Then we make a brief theoretical analysis for the mechanism of rectification. We have equations of motion:

$$\ddot{x}_i = -\frac{\partial V_i(x_i)}{\partial x_i} - \sum_{j=1}^{k_i} \frac{\partial V_j(x_j)}{\partial x_i}, \quad (11)$$

where the first and second terms in the right-hand side of Eq. (11) come from the potentials of node i and its neighbors, respectively. Substituting Eq. (3) into Eq. (11), one has

$$\ddot{x}_i = -\sum_{j=1}^{k_i} C_{i,j} [(x_i - x_j) + \varepsilon(x_i - x_j)^3]. \quad (12)$$

When both the amplitude of x_i and ε ($\varepsilon = 0.1$) are small, we may neglect the nonlinear term in Eq. (12) and obtain

$$\ddot{x}_i = \sum_{j=1}^{k_i} C_{i,j} (x_j - x_i). \quad (13)$$

Equation (13) has plane wave solutions $x_i = e^{I(q_i z_i - \omega_i t_i)}$ and $x_j = e^{I(q_j z_j - \omega_j t_j)}$, where I represents the imaginary unit. Substituting x_i and x_j into Eq. (13), we can obtain the relationship between ω_i and k_i as

$$\omega_i = \sqrt{\sum_{j=1}^{k_i} C_{i,j} [1 - \cos(q_j z_j - q_i z_i + \Theta)]}, \quad (14)$$

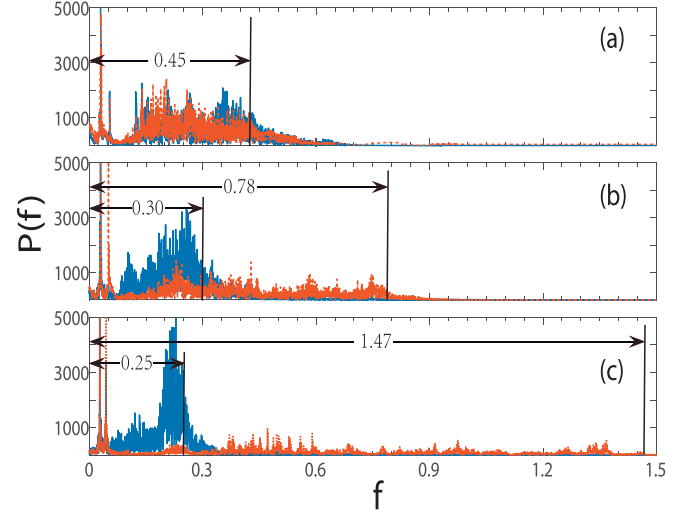


FIG. 7. Case of rewiring both the left and right parts of network. (a–c) Power spectra of the interface nodes with the same degree $k_i = 4$ and $\delta = 0.0$ where the blue and red lines represent the left and right interface nodes, respectively. Panels (a)–(c) represent the cases of $\lambda = 0.0, 0.5$, and 1.0 , respectively.

where $\Theta = \omega_i t_i - \omega_j t_j$ is a constant. Thus, we obtain the range of frequency $f_i = \omega_i / 2\pi$ as

$$0 < f_i < \frac{1}{\pi} \sqrt{\frac{1}{2} \sum_{j=1}^{k_i} r_{i,j}^{-\lambda}}. \quad (15)$$

From Eq. (15) we see that the bandwidth of frequency is controlled by λ . For the case of Fig. 6, i.e., the random network and 2D regular lattice with half by half in Figs. 3(c) and 3(d), the bandwidth of the left interface node will increase when λ decreases. The ranges of the arrows in Fig. 6 show the theoretical results calculated by Eq. (15). We see that the theoretical results are consistent with the power spectra in both Figs. 6(a) and 6(b), indicating that the theory of phonon spectra explains the effect of rectification very well.

Now we move to the case of Fig. 5(a) and 5(b), i.e., the case of rewiring both the left and right parts of network. Figures 7(a)–7(c) show the power spectra of $\delta = 0.0$ where panels (a)–(c) represent the cases for $\lambda = 0.0, 0.5$, and 1.0 , respectively. We also see that the match or mismatch of the power spectra between the two coupled interface nodes controls the heat flux. In Fig. 7(a) with $\lambda = 0.0$, the phonon spectra of the two interface nodes are overlapped with each other perfectly, and thus the heat flux can easily go through the network. However, with the increase of λ , the phonon spectrum of the left interface node becomes narrower, while that of the right interface node becomes wider [see Figs. 7(b) and 7(c)]. Therefore, the rectification effect will be enhanced when λ increases. The ranges of the arrows in Fig. 7(a)–7(c) show the theoretical results calculated by Eq. (15). We see that the theoretical results are also consistent with the power spectra in all the three panels of Fig. 7, confirming again that the theory of phonon spectra can explain the effect of rectification.

V. CONCLUSION AND DISCUSSION

In this work, we have studied the thermal conduction and rectification in a specific asymmetric network rewired from a 2D regular lattice. In this model, each rewired link is implemented according to the probability $P_{i,j} \sim r_{i,j}^{-\delta}$, indicating that a larger δ will result in a shorter average distance. Further, we assume that the coupling strength of each link i, j depends on the distance between the connected nodes i and j by the form of $C_{i,j} = r_{i,j}^{-\lambda}$, indicating that a larger λ will have a smaller coupling strength. Due to the fast development of nanotechnology, it is now very easy to fabricate or grow nanotube or nanowire networks in laboratory [18,52,53]. In this sense, adjusting the two parameters δ and λ will be equivalent to controlling the average length of nanowires and thermal conductivity in real nanonetworks.

Furthermore, we have shown that both parameters δ and λ can influence the heat flux of networks and induce a rectification effect. In particular, there is an optimal λ where the heat flux J_{\pm} will reach their maxima. As nanonetworks have great potential applications in many fields [54,55], the results obtained in this work may provide some highlights in controlling heat conduction. For examples, we may choose the

network structure with smaller J_{\pm} to make thermal devices so that the heat dissipation will not be a serious problem. We may also choose the network structure with larger R_e to make glass windows so that the window will function as a natural air conditioner to keep a warmer room in the winter and a cooler room in the summer by overturning the windows.

In conclusion, we have presented a model of complex networks rewired from a 2D regular lattice to study thermal conduction and rectification in the nanotube or nanowire networks. Our results show that both J_{\pm} and R_e can be manipulated by adjusting the two parameters δ and λ . A brief theoretical analysis of phonon spectra is used to explain the numerical results.

ACKNOWLEDGMENTS

This work was partially supported by the NNSF of China under Grants No. 11675056 and No. 11835003, the Candidate Talents Training Fund of Yunnan Province (Project No. 2015HB025 and No. 11665014), and the Natural Science Foundation of Yunnan Province (Grant No. 2017FB003).

-
- [1] D. Ma, H. Ding, H. Meng, L. Feng, Y. Wu, J. Shiomi, and N. Yang, *Phys. Rev. B* **94**, 165434 (2016).
 - [2] H. Ding, G. Peng, S. Mo, D. Ma, S. W. Sharshir, and N. Yang, *Nanoscale* **9**, 19066 (2017).
 - [3] S. Hu, M. An, N. Yang, and B. Li, *Small* **13**, 1602726 (2016).
 - [4] Q. Song, M. An, X. Chen, Z. Peng, J. Zang, and N. Yang, *Nanoscale* **8**, 14943 (2016).
 - [5] N. B. Li, J. Ren, L. Wang, G. Zhang, P. Hanggi, and B. W. Li, *Rev. Mod. Phys.* **84**, 1045 (2012).
 - [6] S. Lepri, R. Livi, and A. Politi, *Phys. Rep.* **377**, 1 (2003).
 - [7] G. Casati, J. Ford, F. Vivaldi, and W. M. Visscher, *Phys. Rev. Lett.* **52**, 1861 (1984).
 - [8] S. Lepri, R. Livi, and A. Politi, *Phys. Rev. Lett.* **78**, 1896 (1997).
 - [9] B. Li, L. Wang, and G. Casati, *Phys. Rev. Lett.* **93**, 184301 (2004).
 - [10] W. R. Zhong, W. H. Huang, and X. R. Deng *et al.*, *Appl. Phys. Lett.* **99**, 193104 (2011).
 - [11] L. Wang and B. Li, *Phys. Rev. Lett.* **99**, 177208 (2007).
 - [12] Y. Dubi, and D. V. Massimiliano, *Rev. Mod. Phys.* **83**, 131 (2011).
 - [13] B. Li, L. Wang, and G. Casati, *Appl. Phys. Lett.* **88**, 143501 (2006).
 - [14] P. Ben-Abdallah and S. A. Biehs, *Phys. Rev. Lett.* **112**, 044301 (2014).
 - [15] C. Guo, K. Wang, and E. Zerah-Harush *et al.*, *Nat. Chem.* **8**, 484 (2016).
 - [16] H. Wang, S. Hu, and K. Takahashi *et al.*, *Nat. Commun.* **8**, 15843 (2017).
 - [17] M. Terraneo, M. Peyrard, and G. Casati, *Phys. Rev. Lett.* **88**, 094302 (2002).
 - [18] C. W. Chang, D. Okawa, A. Majumdar, and A. Zettl, *Science* **314**, 1121 (2006).
 - [19] H. Yan, S. H. Park, and G. Finkelstein *et al.*, *Science* **301**, 1882 (2003).
 - [20] D. Liu, S. H. Park, and J. H. Reif *et al.*, *Proc. Natl Acad. Sci. USA* **101**, 717 (2004).
 - [21] C. Lin, Y. Ke, and Y. Liu *et al.*, *Angew. Chem. Int. Ed.* **46**, 6089 (2007).
 - [22] P. Yin, R. F. Hariadi, and S. Sahu *et al.*, *Science* **321**, 824 (2008).
 - [23] D. Nykypanchuk, M. M. Maye, and D. L. D. Van *et al.*, *Nature (London)* **451**, 549 (2008).
 - [24] M. Endo and H. Sugiyama, *Chem. Bio. Chem.* **10**, 2420 (2009).
 - [25] R. K. Joshi, L. West, A. Kumar, N. Joshi, S. Alwarappan, and A. Kumar, *Nanotechnology* **21**, 185604 (2010).
 - [26] T. J. Bandy, A. Brewer, and J. R. Burns *et al.*, *Chem. Soc. Rev.* **40**, 138 (2011).
 - [27] C. C. Chien, K. A. Velizhanin, and Y. Dubi *et al.*, *Nanotechnology* **24**, 095704 (2013).
 - [28] S. Behnia and R. Panahinia, *Phys. Lett. A* **381**, 2077 (2017).
 - [29] B. Y. Lee, M. G. Sung, and H. Lee *et al.*, *NPG Asia Mater.* **2**, 103 (2010).
 - [30] Q. Cao and J. A. Rogers, *Adv. Mater.* **21**, 29 (2009).
 - [31] D. R. Kauffman and A. Star, *Angew. Chem. Int. Ed.* **47**, 6550 (2008).
 - [32] D. Stauffer, and A. Aharony, *Introduction to Percolation Theory* (Taylor and Francis, London, 1992).
 - [33] F. Liljeros, C. R. Edling, and L. A. Amaral *et al.*, *Nature (London)* **411**, 907 (2001).
 - [34] R. Albert and A. L. Barabási, *Rev. Mod. Phys.* **74**, 47 (2002).
 - [35] V. Colizza, R. Pastor-Satorras, and A. Vespignani, *Nat. Phys.* **3**, 276 (2007).
 - [36] S. Kumar, J. Y. Murthy, and M. A. Alam, *Phys. Rev. Lett.* **95**, 066802 (2005).
 - [37] E. Lopez, S. V. Buldyrev, S. Havlin, and H. E. Stanley, *Phys. Rev. Lett.* **94**, 248701 (2005).
 - [38] Z. Wu, L. A. Braunstein, S. Havlin, and H. E. Stanley, *Phys. Rev. Lett.* **96**, 148702 (2006).

- [39] Z. Liu and B. Li, *Phys. Rev. E* **76**, 051118 (2007).
- [40] Z. Liu, X. Wu, H. Yang, N. Gupte, and B. Li, *New J. Phys.* **12**, 023016 (2010).
- [41] K. Xiong, C. Zeng, Z. Liu, and B. Li, *Phys. Rev. E* **98**, 022115 (2018).
- [42] R. S. Prasher, X. J. Hu, Y. Chalopin, N. Mingo, K. Lofgreen, S. Volz, F. Cleri, and P. Keblinski, *Phys. Rev. Lett.* **102**, 105901 (2009).
- [43] S. Nosé, *J. Chem. Phys.* **81**, 511 (1984).
- [44] W. G. Hoover, *Phys. Rev. A* **31**, 1695 (1985).
- [45] D. J. Watts and S. H. Strogatz, *Nature (London)* **393**, 440 (1998).
- [46] J. M. Kleinberg, *Nature (London)* **406**, 845 (2000).
- [47] M. Barthélemy, *Phys. Rep.* **499**, 1 (2010).
- [48] L. K. Gallos, H. A. Makse, and M. Sigman, *Proc. Natl. Acad. Sci. USA* **109**, 2825 (2012).
- [49] B. Li, J. H. Lan, and L. Wang, *Phys. Rev. Lett.* **95**, 104302 (2005).
- [50] N. Yang, X. Xu, G. Zhang, and B. Li, *AIP Adv.* **2**, 041410 (2012).
- [51] C. F. Moukarzel and M. Argollo de Menezes, *Phys. Rev. E* **65**, 056709 (2002).
- [52] E. Pop, D. Mann, J. Cao, Q. Wang, K. Goodson, and H. Dai, *Phys. Rev. Lett.* **95**, 155505 (2005).
- [53] C. W. Chang, D. Okawa, H. Garcia, A. Majumdar, and A. Zettl, *Phys. Rev. Lett.* **101**, 075903 (2008).
- [54] G. Pennelli, M. Totaro, M. Piotto, and P. Bruschi, *Nano Lett.* **13**, 2592 (2013).
- [55] D. Son *et al.*, *Nat. Nanotechnol.* **13**, 1057 (2018).